# Structural and Thermodynamic Behavior of Eukaryotic Initiation Factor 4E in Supramolecular Formation with 4E-Binding Protein 1 and mRNA Cap Analogue, Studied by Spectroscopic Methods

Xu SHEN,[a] Koji TOMOO,[a] Susumu UCHIYAMA,[b] Yuji KOBAYASHI,[b] and Toshimasa ISHIDA*,[a]

*Department of Physical Chemistry, Osaka University of Pharmaceutical Sciences,[a] 4–20–1 Nasahara, Takatsuki, Osaka 569–1094, Japan and Faculty of Pharmaceutical Sciences, Osaka University,[b] 1–6 Yamadaoka, Suita 565–0871, Japan.*
Received May 14, 2001; accepted June 22, 2001

**The structural and thermodynamic behavior of the complex formation of eIF4E with either or both mRNA cap analogue ($m^7$GTP, $m^7$GpppA, or $m^7$GpppG) and 4EBP1 has been investigated by spectroscopic measurements. Although the circular dichroism (CD) spectrum of eIF4E was little affected by the association with any cap analogue, the association constant of eIF4E with $m^7$GpppA/G, estimated from the fluorescence quenching, was about 10 times larger than that with $m^7$GTP. The van't Hoff analyses showed that the $m^7$GpppA/G binding is enthalpy-driven with a large negative $\Delta H°$, and this is in contrast with the entropy-driven binding of $m^7$GTP, where the positive $\Delta S°$ is large enough to overcome an increase of $\Delta H°$. This different behavior obviously originates in the interaction of the second nucleotide in $m^7$GpppA with eIF4E, suggesting the importance of the nucleotide sequence linked to the $m^7$Gppp terminal moiety, in addition to the specific interaction with the $m^7$G base, for the recognition of mRNA cap structure by eIF4E. On the other hand, the CD spectra indicated that the binding of 4EBP1, an endogenous eIF4E-regulatory protein without having any defined secondary structure, shifted the $m^7$GTP- or $m^7$GpppA/G-bound eIF4E to an irregular structure, although such a structural change was not observed for eIF4E alone. The association constant of 4EBP1 with $m^7$GTP- or $m^7$GpppA/G-bound eIF4E was by two orders of magnitude larger than that with eIF4E alone. These results suggest the close interrelation in the supramolecular formation of 4EBP–eIF4E–mRNA cap structure.**

**Key words** eukaryotic initiation factor 4E; mRNA cap structure; 4E-binding protein; supramolecular formation; spectroscopy; thermodynamic parameter

Eukaryotic mRNAs have a common cap structure [$m^7$G(5′)ppp(5′)N, where N is any nucleotide] at the 5′-terminal portion and it plays important roles in stabilizing the mRNA structure and facilitating mRNA binding to ribosome during the initiation.[1)] To allow the efficient translation of mRNA, an interaction is required between the cap structure and eukaryotic initiation factor eIF4F, consisting of eIF4A, eIF4G and eIF4E.[2)] EIF4E, the smallest subunit in eIF-4F, binds specifically to the mRNA cap structure and catalyzes the first step of protein synthesis. Furthermore, it has been indicated that the translation by eIF4E is regulated through the interaction with endogenous 4E-binding protein (4EBP1, 4EBP2 and 4EBP3) and the interrelated phosphorylation of eIF4E and 4EBPs. The structural function of 4EBP has little or no folded structure, and the sequence of residues 49—68 is sufficient to bind with eIF4E and to inhibit its translation in reticulocyte lysate.[3)]

The respective biological functions of eIF4E, mRNA cap structure, and 4EBP have been well investigated. However, studies on the physicochemical properties in the supramolecular formation of these molecules are few, although these data are important to understand the regulation mechanism of eIF4E in the translation initiation at the molecular level. Bearing this in mind, we have been investigating the binding behavior of supramolecular formation of eIF4E with mRNA cap structure and 4EBP1.[4,5)]

$m^7$GDP or $m^7$GTP usually has been used as a model representing the functional property of mRNA cap structure. However, our preliminary spectroscopic data showed a notable difference between the interactions of eIF4E with $m^7$GpppA or $m^7$GpppG (hereafter abbreviated as $m^7$GpppA/G) and $m^7$GTP, especially in the thermodynamic behaviors of the respective complexes. Since $m^7$GpppA/G could reflect more closely the feature of mRNA cap structure than $m^7$GTP, the delineation of such different interaction appears important in considering the structural basis for the mutual regulation in the supramolecular formation among 4EBP, eIF4E, and mRNA cap structure.

## Experimental

**Materials** The enzymes for the preparation of recombinant proteins were purchased from Takara Shuzo, New England Biolabs Inc., Toyobo Co., Bethesda Research Laboratories, P-L Biochemicals, or Novagen Co. The bacterial strain BL21 (DE3) (Novagen) was used for the transformation. The $m^7$GTP- and glutathione–sepharose 4B affinity resins were purchased from Pharmacia Biotechnology Inc. The markers for molecular weight estimation were obtained from BioRad Co. Other commercially available materials were of reagent grade or higher.

**Preparation of Recombinant $m^7$GTP- or $m^7$GpppA/G-Free and -Bound eIF4Es** The expression of recombinant human eIF4E in *Escherichia coli* and its isolation were carried out according to previously published methods.[6,7)] The purification of recombinant eIF4E and its complex with $m^7$GTP or $m^7$GpppA/G was performed according to the method of Morino *et al*.[8)] The supernatant was applied to a $m^7$GTP-Sepharose 4B affinity column equilibrated with buffer A (20 mM HEPES–KOH, pH 7.5, 1 mM DTT (dithiothreitol), 0.1 mM EDTA, 100 mM KCl), and the column was washed with buffer A until the optical density returned to the baseline. The bound materials were then eluted with buffer B (buffer A+0.1 mM $m^7$GTP or 0.1 mM $m^7$GpppA/G), leading to the solution of eIF4E–$m^7$GTP or –$m^7$GpppA/G complex. After purification by gel filtration, the purity was confirmed by SDS-PAGE (sodium dodecylsulfate polyacrylamide gel electrophoresis). The fractions were concentrated with a centricon 10 (Amicon Co.) to an expected concentration for the experimental use. The cap-free eIF4E was prepared by the elution of eIF4E bound to the affinity column using buffer A containing 1 M KCl, instead of 100 mM KCl.

**Preparation of GST-Fused 4EBP1 and Isolation of 4EBP1** The gene expression of recombinant human GST-fused 4EBP1 protein in *E. coli* was performed according to the previous method.[4)] The supernatant was applied to a glutathione–Sepharose 4B affinity column equilibrated with buffer C

* To whom correspondence should be addressed. e-mail: ishida@oysun01.oups.ac.jp

(50 mM Tris–HCl, pH 8.0, 1 mM EDTA) and the column was washed with the same buffer until the optical density of the eluted buffer returned to the baseline level. After the GST-4EBP1-bound column was equilibrated with buffer D (20 mM Tris–HCl, pH 8.0, 150 mM NaCl) including 2.5 mM $CaCl_2$ containing 0.5% thrombin at 25 °C for 3 h, the eluate was collected. The column was then washed with buffer D, and the eluate was combined and purified by Mono-Q ion exchange column and a Sephadex G-75 gel filtration system. Finally, a benzamidine–Sepharose 6B column was used to remove thrombin as completely as possible.

**Preparation of 4EBP1–eIF4E–m$^7$GTP or –m$^7$GpppA/G Ternary Complex** The m$^7$GTP-bound eIF4E affinity column (as stated above) was equilibrated with the 4EBP1 solution (the molar ratio of 4EBP1 : eIF4E = around 3 : 1) for about 1 h at 25 °C, washed with buffer A thoroughly until the optical density returned to the baseline, and then eluted with buffer B. The purified 4EBP1–eIF4E–m$^7$GTP or m$^7$GpppA/G complex was obtained through gel filtration. The purity of the prepared complex was checked by SDS-PAGE.

**Circular Dichroism (CD) Spectroscopy** The sample solutions were adjusted to 10 $\mu$M concentration by phosphate buffer (10 mM sodium phosphate, pH 7.0, 1 mM EDTA) through dialysis. CD spectra were measured using a JASCO-720 spectropolarimeter, reading in the region of 200—260 nm, with a scan speed of 20 nm/min, sensitivity of 20 mdeg, in a quartz cell of 1 mm path length. The temperature dependence of CD spectrum was investigated in the range of 4—90 °C. m$^7$GTP or m$^7$GpppA itself did not exhibit any CD spectra in the region of 200—260 nm.

**Fluorescence Spectroscopy** Fluorescence spectra were measured on a JASCO FP-770F with a 10-mm cell. Measurements of the emission spectra (290 nm excitation) were carried out in buffer A (10 $\mu$M concentration) at different temperatures (4, 10, 20, 30 °C). The emission and excitation slits were set at 10 nm. The association constants (K) of eIF4E with mRNA cap analogue or 4EBP1, or its ternary complex were obtained from the slope of Eadie–Hofstee plot[9] by least squares linear analysis:

$$\Delta F = \frac{1}{K}\frac{\Delta F}{[\text{cap analogue or 4EBP1}]} + \Delta F_c$$

where $\Delta F$ is the difference of fluorescence between the eIF4E free and coexisted with mRNA cap analogue or 4EBP1 at the concentration of [cap analogue] or [4EBP1], respectively, and $\Delta F_c$ is the difference of fluorescence between the eIF4E free and completely complexed with cap analogue or 4EBP1.

## Results and Discussion

**CD Spectral Feature of eIF4E Complexed with Cap Structure and/or 4EBP1** The CD spectra of 4EBP1, eIF4E, and their complexes in the absence and presence of m$^7$GTP or m$^7$GpppA are shown in Fig. 1. Since the effects of m$^7$GpppA and m$^7$GpppG on CD spectra of eIF4E and 4EBP1 were nearly the same, only the former cap analogue is discussed here, except for a special case. The CD spectra could be divided into two patterns, *i.e.*, group I (eIF4E, eIF4E–m$^7$GTP, eIF4E–m$^7$GpppA, 4EBP1–eIF4E) and group II (4EBP1, 4EBP1–eIF4E–m$^7$GTP, 4EBP1–eIF4E–m$^7$GpppA). The spectra of group I are characterized by a minimum peak at 209 and a negative shoulder at 222 nm and indicate the existence of a partial $\alpha$-helical structure in eIF4E and its complex with m$^7$GpppA, m$^7$GTP, or 4EBP1. In contrast, no notable secondary structure is suggested for group II, *i.e.*, 4EBP1 and its complex with eIF4E–m$^7$GTP or –m$^7$GpppA (hereafter noted as an irregular structure), although two hollow curves at 205 and 222 nm (a very shallow shoulder) in 4EBP1–eIF4E–m$^7$GTP and 4EBP1–eIF4E–m$^7$GpppA may reflect a trace of helical structure. It is interesting to note that the $\alpha$-helical component of eIF4E in the 4EBP1–eIF4E or eIF4E–cap analogue complex is converted to an irregular structure by the ternary complex formation with the cap structure or 4EBP1, respectively. This could be interpreted as either i) the secondary structure of eIF4E complexed with a cap structure is transformed into an irregular structure by the binding of 4EBP1 or ii) the binding of mRNA cap structure acts as a trigger for the deformation of eIF4E secondary structure in 4EBP1–eIF4E complex. In any case, this indicates the close interplay between the 4EBP1 and cap structure with respect to eIF4E, and does not conflict with previous reports,[5,10] in which the binding of 4EBP was shown to transform the structure of eIF4E into a high cap-affinity state.

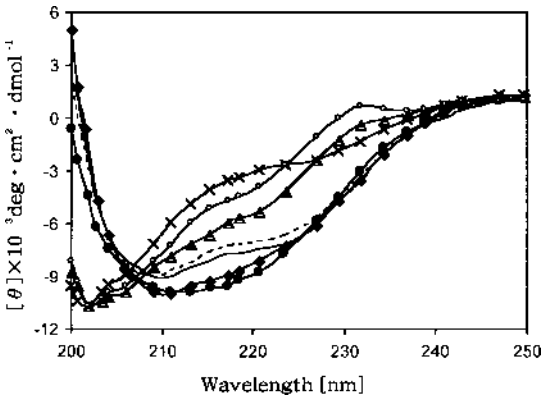


Fig. 1. CD Spectra of 4EBP1, m$^7$GTP/m$^7$GpppA-Free or -Bound eIF4E, and Their Complexes at 4 °C

4EBP1 (—×—×—), eIF4E-free (——), eIF4E–m$^7$GTP (—◆—◆—), eIF4E–m$^7$GpppA (—●—●—), 4EBP1–eIF4E (------), 4EBP1–eIF4E–m$^7$GTP (—○—○—), 4EBP1–eIF4E–m$^7$GpppA (—△—△—).

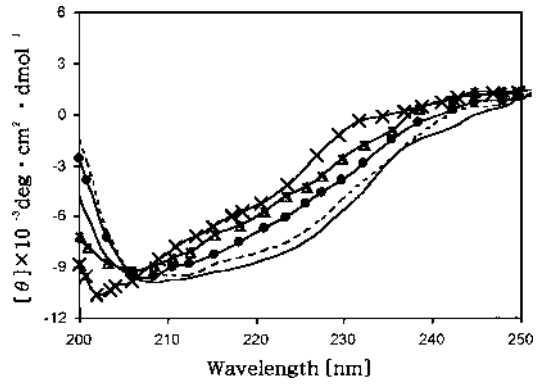


Fig. 2. CD Spectra of 4EBP1–eIF4E–m$^7$GpppA Complex at Different Temperature

—×—×— (4 °C), —●—●— (60 °C), ------ (70 °C), —— (90 °C), —△—△— (after being heated to 90 °C, cooled down to 4 °C). The respective samples were held for 15 min before being measured.

**Thermal Stability of Complex by CD Spectral Change** Thermal behaviors of these proteins and their complexes were examined by the temperature-dependence of CD spectral changes. The result for 4EBP1–eIF4E–m$^7$GpppA is shown in Fig. 2. Nearly the same profile was observed for 4EBP1–eIF4E–m$^7$GTP. Provided that the negative CD curve at 220—230 nm reflects the signal of any secondary structure such as $\alpha$-helical structure, the CD change at about 60 °C is indicative of the dissociation of eIF4E from the complex, because the spectrum at >60 °C is very similar to that of eIF4E alone. From comparison of CD spectra at 4 °C before and after heating to 90 °C, it could be said that the conformation of eIF4E in the complex is to some extent reversible between groups I and II.

On the other hand, the thermal CD change for eIF4E–m$^7$GpppA complex is shown in Fig. 3. Similar temperature-

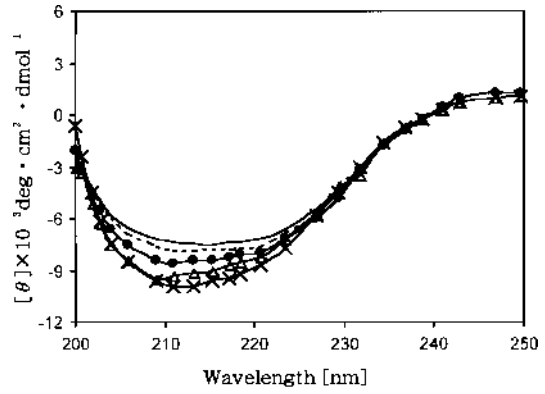


Fig. 3. CD Spectra of eIF4E–m$^7$GpppA Complex at Different Temperature

—×—×— (4 °C), —●—●— (60 °C), ------ (70 °C), —— (90 °C), —△—△— (after being heated to 90 °C, cooled down to 4 °C). The respective samples were held for 15 min before being measured.

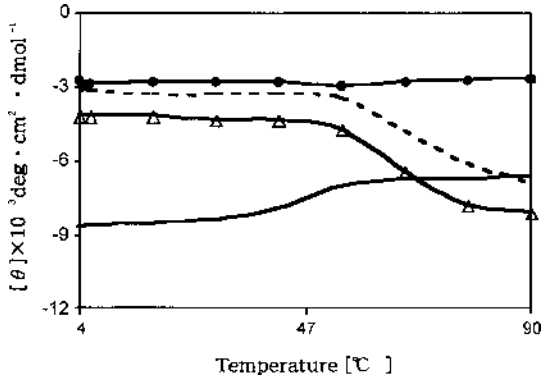


Fig. 4. Temperature Dependence of Ellipticities of 4EBP1, m$^7$GTP/m$^7$GpppA-Free or -Bound eIF4E, and Their Complexes at 222 nm

4EBP1 (—●—●—), eIF4E–m$^7$GpppA (——), 4EBP1–eIF4E–m$^7$GTP (------), 4EBP1–eIF4E–m$^7$GpppA (—△—△—). The thermal profiles of eIF4E-free, eIF4E–m$^7$GTP and 4EBP1–eIF4E were almost overlapped that of eIF4E–m$^7$GpppA. The heating rate was 0.1 deg/min.

dependent CD profiles were observed for eIF4E free and its complexes in group I. The CD spectra at 4 °C before and after heating to 90 °C indicated that the secondary structural component of eIF4E is reversibly recovered from the thermal denaturation. The component decreases linearly with the rise of temperature until about 60 °C, and almost the original state is recovered without any conformational transition as temperature lowers. This is in contrast to the case of group II (Fig. 2), indicating that the thermal behavior of eIF4E structure is different between the ternary and binary complexes.

To monitor the thermal behavior of eIF4E and its binary or ternary complex, the CD ellipticities at 222 nm of 4EBP1, eIF4E–m$^7$GTP, eIF4E–m$^7$GpppA, and 4EBP1–eIF4E–m$^7$GpppA were measured as a function of temperature and results are shown in Fig. 4, where the case of 4EBP1 is also shown for comparison. Concerning 4EBP1–eIF4E–m$^7$GpppA ternary complex, the ellipticity at 222 nm begins to decrease from about 60 °C; similar change was observed for 4EBP1–eIF4E–m$^7$GTP complex. In contrast, the curves of eIF4E–4EBP1 and eIF4E–m$^7$GpppA complexes showed opposite profiles, *i.e.*, their ellipticities began to increase from about 30 °C and to reach a plateau at about 60 °C, where both complexes had an apparent $T_m$ value of 48 °C.

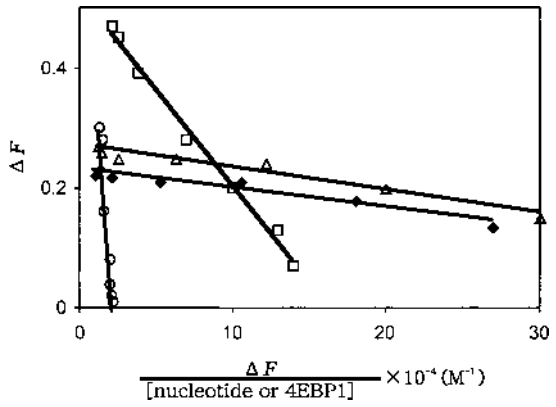


Fig. 5. Eadie–Hofstee Plots of eIF4E with m$^7$GTP/m$^7$GpppA, 4EBP1, and Their Complexes at 4 °C

eIF4E–m$^7$GTP (—□—□—), eIF4E–m$^7$GpppA (—△—△—), 4EBP1–eIF4E (—○—○—), 4EBP1–eIF4E–m$^7$GpppA (—◆—◆—). The solid lines are the least-squares fits for the respective data. $\Delta F$ shows the quenching of the fluorescence. The concentration for the cap analogue or 4EBP1 was varied at 0.5, 1.0, 2.0, 4.0, 10.0, 18.0, and 22 $\mu$M. EIF4E was used at the concentration of 5 $\mu$M. The plot of 4EBP1–eIF4E–m$^7$GTP was almost the same as that of 4EBP1–eIF4E–m$^7$GpppA and is thus omitted.

Apparently, the different binding process, *i.e.* the binding of 4EBP1 to eIF4E–m$^7$GpppA and that of m$^7$GpppA to 4EBP1–eIF4E, causes this notable difference. This also implies that the structural/functional behavior of eIF4E in the binary complex (eIF4E–m$^7$GpppA or 4EBP1–eIF4E) is significantly influenced by the ternary complex formation with 4EBP1 or m$^7$GpppA, as was already stated in the previous section. In summary, the secondary structure of eIF4E in the ternary complex could be said to reversibly begin to change at >60 °C, whereas in the case of binary complex, the secondary structural moiety in eIF4E begins to deform from 40 °C and remains unchanged beyond about 60 °C.

**EIF4E–Cap Analogue Interaction by Fluorescence Measurements: Importance of the Second Nucleotide of m$^7$GpppA/G for Interaction** Because of eight Trp residues are contained in eIF4E, the fluorescence spectroscopy has often been used as a tool to monitor the interaction between the cap analogue and eIF4E.[6,11] The interactions with m$^7$GTP and m$^7$GpppA were compared to determine the contribution of the second nucleotide of m$^7$GpppA/G to the interaction with eIF4E. Their association constants were estimated from the respective slopes of Eadie–Hofstee plots (Fig. 5, Table 1). From the temperature dependence of these association constants, the thermodynamic parameters for the respective complexes were estimated (Table 2). Assuming that the process is accompanied by no remarkable change in heat capacity, the $\Delta H$ value is obtained by least-squares from the slope of van't Hoff equation ($\ln K = -\Delta H/(\boldsymbol{RT}) + \Delta S/\boldsymbol{R}$). Since the plot of $\ln K$ *vs.* $1/T$ gave a straight line (correlation coefficient of >0.95) for each of the complexes, $\Delta H$ would be independent of temperature in the range of 4—30 °C. The $\Delta G°$ and $\Delta S°$ values at 25 °C were calculated from $\Delta G° = -\boldsymbol{RT}\ln K$ and $\Delta G° = \Delta H° - T\Delta S°$, respectively.

As is obvious from the tables, the association of m$^7$GpppA/G with eIF4E is about 10 times as large as that of m$^7$GTP. This is in contrast to the published data,[12,13] where the binding preference of m$^7$GTP over m$^7$GpppA/G was observed. The reasons for the discrepancies between these re-

Table 1. Association Constants of eIF4E with $m^7$GTP or $m^7$GpppA/G, and of 4EBP1 with eIF4E, eIF4E–$m^7$GTP, or –$m^7$GpppA/G Complex

| Complex | Ka/M$^{-1}$ at 4 (°C) | Ka/M$^{-1}$ at 10 (°C) | Ka/M$^{-1}$ at 20 (°C) | Ka/M$^{-1}$ at 30 (°C) |
|---|---|---|---|---|
| eIF4E–$m^7$GTP | $(2.18\pm0.13)\times10^5$ | $(2.27\pm0.11)\times10^5$ | $(2.33\pm0.15)\times10^5$ | $(2.54\pm0.31)\times10^5$ |
| eIF4E–$m^7$GpppA | $(2.33\pm0.37)\times10^6$ | $(2.22\pm0.27)\times10^6$ | $(1.14\pm0.18)\times10^6$ | $(8.77\pm0.30)\times10^5$ |
| eIF4E–$m^7$GpppG | $(5.55\pm0.26)\times10^6$ | $(3.85\pm0.44)\times10^6$ | $(2.43\pm0.31)\times10^6$ | $(1.39\pm0.20)\times10^6$ |
| 4EBP1–eIF4E | $(3.25\pm0.14)\times10^4$ | $(3.64\pm0.25)\times10^4$ | $(4.22\pm0.19)\times10^4$ | $(5.08\pm0.12)\times10^4$ |
| 4EBP1–eIF4E–$m^7$GTP | $(3.33\pm0.21)\times10^6$ | $(3.70\pm0.36)\times10^6$ | $(4.45\pm0.41)\times10^6$ | $(5.29\pm0.37)\times10^6$ |
| 4EBP1–eIF4E–$m^7$GpppA | $(3.12\pm0.18)\times10^6$ | $(4.17\pm0.48)\times10^6$ | $(4.35\pm0.33)\times10^6$ | $(5.44\pm0.24)\times10^6$ |
| 4EBP1–eIF4E–$m^7$GpppG[a] | $(3.48\pm0.37)\times10^6$ | $(4.02\pm0.25)\times10^6$ | $(4.79\pm0.50)\times10^6$ | $(5.12\pm0.42)\times10^6$ |

*a*) The difference of the association constant previously reported for eIF4E–$m^7$GpppG ($3.89\times10^5$ at 23 °C)[7] from the present value could have resulted from a different preparation of the eIF4E sample. In the previous study, the sample was prepared by the solubilization, renaturation, and ion exchange/gel chromatography of eIF4E expressed as an insoluble form, and the cap-binding ability of the sample appears to be inferior to the present sample, prepared by cap-affinity chromatography of the soluble recombinant eIF4E.

Table 2. Thermodynamic Binding Parameters of eIF4E with $m^7$GTP or $m^7$GpppA/G, and of 4EBP1 with eIF4E, eIF4E–$m^7$GTP, or eIF4E–$m^7$GpppA/G Complex at 25 °C

| Complex | $\Delta H°$ (kJ·mol$^{-1}$) | $\Delta S°$ (J·mol$^{-1}$K$^{-1}$) | $\Delta G°$ (kJ·mol$^{-1}$) |
|---|---|---|---|
| eIF4E–$m^7$GTP | $3.90\pm0.35$ | $116.23\pm0.28$ | $-30.74\pm1.40$ |
| eIF4E–$m^7$GpppA | $-30.06\pm0.48$ | $14.27\pm0.35$ | $-34.31\pm0.91$ |
| eIF4E–$m^7$GpppG | $-36.42\pm0.24$ | $-2.30\pm0.29$ | $-35.73\pm1.70$ |
| 4EBP1–eIF4E | $11.89\pm0.25$ | $129.27\pm0.41$ | $-26.63\pm0.18$ |
| 4EBP1–eIF4E–$m^7$GTP | $12.62\pm0.17$ | $170.36\pm0.22$ | $-38.15\pm0.77$ |
| 4EBP1–eIF4E–$m^7$GpppA | $13.06\pm0.29$ | $172.02\pm0.50$ | $-38.20\pm1.23$ |
| 4EBP1–eIF4E–$m^7$GpppG | $10.59\pm0.31$ | $163.68\pm0.45$ | $-38.19\pm0.80$ |

sults and ours are not known at present. But the binding preference of $m^7$GpppA/G over $m^7$GTP was also supported by the comparative experiment of their elution abilities of eIF4E bound to a cap-affinity column. Furthermore, the crystal structure of human eIF4E–$m^7$GppppA complex (Tomoo *et al*., unpublished data) showed the interaction of the A nucleotide with Thr203–Ser209 region in eIF4E, leading to the conformational stability of this region. These facts suggest the importance of the second nucleotide for the interaction with eIF4E.

Although the $\Delta G°$ value for the binding of $m^7$GpppA/G to eIF4E was almost the same as that to $m^7$GTP, the data suggest different forces driving the interaction. The binding of $m^7$GpppA/G could occur as enthalpy-driven with large negative $\Delta H°$ and small positive or negative $\Delta S°$, whereas that of $m^7$GTP could be entropy-driven with large positive $\Delta S°$ and small positive $\Delta H°$, leading to a negative $\Delta G°$ (Table 2). It would be interpretable from this result that the structure of the eIF4E–$m^7$GpppA/G complex is more tightly packed than that of eIF4E–$m^7$GTP. The X-ray crystal structure of the eIF4E mutant–$m^7$GDP complex[14] showed that the cap-binding domain in eIF4E becomes flexible by the binding of $m^7$G base, reflecting the large increase of positive $\Delta S°$ by the binding of $m^7$GTP. Thus, the additional interaction of the second A/G nucleotide with eIF4E contributes importantly in forming a tightly packed structure in the eIF4E–$m^7$GpppA/G complex. On the other hand, the thermodynamic parameters indicate a different contribution between the second nucleotides A and G to the interaction with eIF4E. The latter could contribute more efficiently to the formation of the ordered complex structure than the former, although the $\Delta G°$ values for the complex formation are almost the same.

**Interaction of 4EBP1 with eIF4E–$m^7$GTP and eIF4E–$m^7$GpppA/G Complexes** The fluorescence of Trp residues in eIF4E is very sensitive to the interaction with 4EBP1, despite the fact that these residues are not located at the binding region of 4EBP.[15] Thus, the association constants of 4EBP1–eIF4E, 4EBP1–eIF4E-$m^7$GTP, and 4EBP1–eIF4E–$m^7$GpppA/G and their thermodynamic parameters were measured based on the respective fluorescence changes. These data are also given in Tables 1 and 2; the association constants of 4EBP1 with the cap-bound eIF4E were essentially the same as those of $m^7$GTP or $m^7$GpppA/G with the 4EBP1-bound eIF4E. The data showed that, while the binding of 4EBP1 to eIF4E alone is relatively weak, its binding to the $m^7$GTP or $m^7$GpppA/G-bound eIF4E increases by almost two orders; this result is comparable to previous results by the surface plasmon resonance (SPR) method.[5,16] In contrast to the interaction of eIF4E with the cap structure, the bindings of 4EPB1 to eIF4E–$m^7$GTP and eIF4E–$m^7$GpppA/G are both entropy-driven with similar negative $\Delta G°$ values. This means that there is no structural difference between eIF4E–$m^7$GTP and eIF4E–$m^7$GpppA/G binary complexes concerning the tertiary complex formation with 4EBP1. In other words, the binding of 4EBP1 shifts the binding state of eIF4E with $m^7$GpppA/G to the same situation as that with $m^7$GTP.

The tertiary structure of eIF4E showed a dorsal relationship between the 4EBP and cap binding pockets.[14,17] Thus, the present results could be explained by the allosteric behavior of eIF4E, the tertiary structure of which is changed to a high 4EBP- or cap-affinity state by the binding of cap structure or 4EBP, respectively; this interpretation was also proposed by Ptushkina *et al*.[10] On the other hand, the following discussion would also be possible from the present results. The cap-binding pocket of eIF4E, which is indirectly affected by the 4EBP-binding pocket, forms two kinds of cap structure-dependent and thermodynamically different structures, depending on the absence/presence of the second nucleotide in the cap structure. In contrast, the 4EBP-binding pocket, which is significantly affected by the binding of cap structure to the cap-binding pocket, transforms the eIF4E–cap complex to an irregular structure by the binding of 4EBP, the thermodynamic behavior of which becomes uniform in spite of the difference of cap structures. These results are useful in understanding the delicate mutual regulation in the supramolecular formation of 4E-BP–eIF4E–mRNA cap structure.

**Acknowledgements** One of the authors (X. S.) was supported by "a JSPS Postdoctoral Fellowship Program for Foreign Researchers" (ID No. 98445).

**References**

1) Reddy R., Singh R., Shimba S., *Pharmacol. Ther*., **54**, 249—267 (1992).
2) Gingras A. C., Raught B., Sonenberg N., *Annu. Rev. Biochem.*, **68**, 913—963 (1999).
3) Fletcher C. M., McGuire A. M., Gingras A. C., Li H. J., Matsuo H., Sonenberg N., Wagner, G., *Biochemistry*, **37**, 9—15 (1998).
4) Nishi N., Morino S., Tomoo K., Youtani T., Ishida T., *J. Biochem*. (Tokyo), **123**, 157—161 (1998).
5) Youtani T., Tomoo K., Ishida T., Miyoshi H., Miura K., *IUBMB Life*, **49**, 1—5 (2000).
6) Ueda H., Maruyama H., Doi M., Inoue M., Ishida T., Morioka H., Tanaka T., Nishikawa S., Uesugi S., *J. Biochem.* (Tokyo), **109**, 882—889 (1991).
7) Morino S., Yasui M., Inoue M., Ishida T., Ueda H., Uesugi S., *J. Biochem.* (Tokyo), **116**, 687—693 (1994).
8) Morino S., Hazama H., Ozaki M., Teraoka Y., Shibata S., Doi M., Ueda H., Ishida T., Uesugi S., *Eur. J. Biochem*., **239**, 597—601 (1996).
9) Eadie G. S., *J. Biol. Chem*., **146**, 85—92 (1942).
10) Ptushkina M., von der Haar T., Karim M. M., Hughes J. M. X., McCarthy J. E. G., *EMBO J*., **18**, 4068—4075 (1999).
11) Wieczorek Z., Zdanowski K., Chlebicka L., Stepinski J. Jankowska M., Kierdaszuk B., Temeriusz A., Darzynkiewicz E., Stolarski R., *Biochim. Biophys. Acta*, **1354**, 145—152 (1997).
12) Cai A., Jankowska-Anyszka M., Centers A., Chlebicka L., Stepinski J., Stolarski R., Darzynkiewicz E., Rhoads R. E., *Biochemistry*, **38**, 8538—8547 (1999).
13) Wieczorek Z., Niedzwiecka-Kornas A., Chlebicka L., Jankowska M., Kiraga K., Stepinski J., Dadlez M., Drabent R., Darzynkiewicz E., Stolarski R., *Z. Naturforsch*., **54c**, 278—284 (1999).
14) Marcotrigiano J., Gingras A.-C., Sonenberg N., Burley S. K., *Cell*, **89**, 951—961 (1997).
15) Marcotrigiano J., Gingras A.-C., Sonenberg N., Burley S. K., *Mol. Cell*, **3**, 707—716 (1999).
16) Miyoshi H., Youtani T., Ide H., Hori H., Okamoto K., Ishikawa M., Wakiyama M., Nishino T., Ishida T., Miura K., *J. Biochem.* (Tokyo), **126**, 897—904 (1999).
17) Matsuo H., Li H., McGuire A. M., Fletcher C. M., Gingras A. C., Sonenberg N., Wagner G., *Nature Struct. Biol*., **4**, 717—724 (1997).